



# Predicting mild cognitive impairment progression to Alzheimer's disease based on machine learning analysis of cortical morphological features

Wei Wang<sup>1,2</sup> · Jiaxuan Peng<sup>1</sup> · Jie Hou<sup>1</sup> · Zhongyu Yuan<sup>1</sup> · Wutao Xie<sup>2</sup> · Guohe Mao<sup>3</sup> · Yaling Pan<sup>4</sup> · Yuan Shao<sup>4</sup> · Zhenyu Shu<sup>4</sup>

Received: 26 April 2023 / Accepted: 25 May 2023 / Published online: 5 July 2023  
© The Author(s), under exclusive licence to Springer Nature Switzerland AG 2023

## Abstract

**Purpose** To establish a model for predicting mild cognitive impairment (MCI) progression to Alzheimer's disease (AD) using morphological features extracted from a joint analysis of voxel-based morphometry (VBM) and surface-based morphometry (SBM).

**Methods** We analyzed data from 121 MCI patients from the Alzheimer's Disease Neuroimaging Initiative, 32 of whom progressed to AD during a 4-year follow-up period and were classified as the progression group, while the remaining 89 were classified as the non-progression group. Patients were divided into a training set ( $n = 84$ ) and a testing set ( $n = 37$ ). Morphological features measured by VBM and SBM were extracted from the cortex of the training set and dimensionally reduced to construct morphological biomarkers using machine learning methods, which were combined with clinical data to build a multimodal combinatorial model. The model's performance was evaluated using receiver operating characteristic curves on the testing set.

**Results** The Alzheimer's Disease Assessment Scale (ADAS) score, apolipoprotein E (APOE4), and morphological biomarkers were independent predictors of MCI progression to AD. The combinatorial model based on the independent predictors had an area under the curve (AUC) of 0.866 in the training set and 0.828 in the testing set, with sensitivities of 0.773 and 0.900 and specificities of 0.903 and 0.747, respectively. The number of MCI patients classified as high-risk for progression to AD was significantly different from those classified as low-risk in the training set, testing set, and entire dataset, according to the combinatorial model ( $P < 0.05$ ).

**Conclusion** The combinatorial model based on cortical morphological features can identify high-risk MCI patients likely to progress to AD, potentially providing an effective tool for clinical screening.

**Keywords** Mild cognitive impairment · Alzheimer's disease · White matter · Cortical morphology · Machine learning

## Introduction

Alzheimer's disease (AD) is an irreversible degenerative brain disease and the most common type of dementia in the elderly [1]. Currently, there are no effective treatment measures to stop

---

Wei Wang and Jiaxuan Peng have contributed equally to this work.

✉ Zhenyu Shu  
cooljuty@hotmail.com

<sup>1</sup> Jinzhou Medical University Postgraduate Education Base (Zhejiang Provincial People's Hospital, People's Hospital of Hangzhou Medical College), Hangzhou, Zhejiang, China

<sup>2</sup> Department of Radiology, The First Affiliated Hospital of Chongqing Medical and Pharmaceutical College, Chongqing, China

<sup>3</sup> Banan Hospital of Chongqing Medical University, Chongqing, China

<sup>4</sup> Center for Rehabilitation Medicine, Department of Radiology, Zhejiang Provincial People's Hospital, Affiliated People's Hospital, Hangzhou Medical College, No. 158 Shangtang Road, Hangzhou City, Zhejiang Province, China

or reverse the progression of AD [2]. The focus of AD intervention has shifted to the mild cognitive impairment (MCI) stage, which is an intermediate state between normal aging and AD, and has not yet reached the diagnostic criteria for dementia. Among MCI patients, 10% to 15% develop progressive mild cognitive impairment (pMCI), while some maintain their current cognitive level or even reverse to normal, known as stable mild cognitive impairment (sMCI). Early identification and treatment of pMCI may delay or even convert it to sMCI [3], making accurate diagnosis, early intervention, and prognosis prediction of MCI patients particularly important.

MRI is a noninvasive and widely used functional imaging technique in neuroimaging research that has advantages in obtaining both brain structure and function [4]. In a large number of studies on brain structural morphology measurement, cortical atrophy is considered the biological basis of cognitive decline and a sensitive biological marker of AD [5, 6]. At present, the commonly used methods for measuring brain cortical atrophy include voxel-based morphometry (VBM) and surface-based morphometry (SBM). VBM is a widely applicable analysis method that has been used for measuring brain tissue in various neurological diseases [7]. It can accurately obtain voxel-level volume/concentration of gray matter (GM). However, the explanation for subtle changes in cortical structure is considered less reliable. [8]. On the other hand, SBM is not as good as VBM in measuring GM volume [8], but it can quantify changes in cortical structure under physiological and pathological conditions by extracting morphological parameters such as cortical thickness, surface area, and curvature of brain tissue [9]. Therefore, the combination of VBM and SBM may provide a complementary method for detecting cortical morphological changes. In addition, machine learning-based algorithms applied to multimodal data have a great advantage in predicting the progression from MCI to AD [10]. Therefore, this study hypothesizes that morphological features extracted from a joint application of VBM and SBM can help identify pMCI patients, and the combination of machine learning algorithms can improve the efficiency of this identification.

The primary objective of this study was to extract morphological features from the cortical area and use machine learning to construct imaging biomarkers to identify pMCI. Second, based on imaging biomarkers and related clinical features, a combinatorial model will be constructed to predict high-risk MCI patients who may progress to AD.

## Materials and methods

### Demographic data

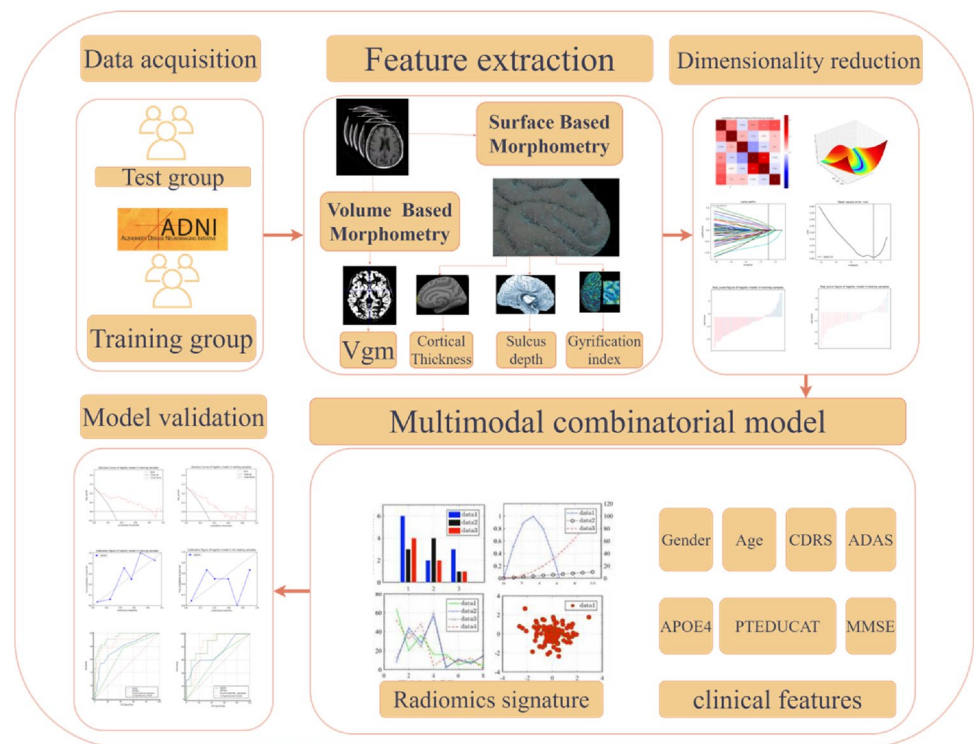
All the cases included in this study were obtained from the Alzheimer's Disease Neuroimaging Initiative (ADNI)

official website ([adni.loni.usc.edu](http://adni.loni.usc.edu)), specifically the ADNI-2 and ADNI-GO datasets. For information on the ethical review of the ADNI data, please refer to the website. The ADNI was launched in 2003 as a \$60 million, 5-year, public–private partnership by the National Institute on Aging, the National Institute of Biomedical Imaging and Bioengineering, the United States Food and Drug Administration (US FDA), private pharmaceutical companies, and nonprofit organizations. A total of 121 patients with a baseline diagnosis of mild cognitive impairment (MCI) were included in this study, of whom 32 progressed to Alzheimer's disease (AD) and were classified as the progression group during the 4-year follow-up period, while the remaining 89 were classified as the non-progression group. According to the time of data entry, these cases were divided into a training set ( $n=84$ ) and a test set ( $n=37$ ), with the training set used to build the model and the test set used to validate its performance, and the details of the study process can be found in Fig. 1. The inclusion criteria were as follows: all patients initially diagnosed with MCI underwent follow-up examination; all patients underwent MRI examination and had complete clinical data. The exclusion criteria mainly included a lack of biological indicators and scale evaluations and patients with conversion phenomena. For detailed information on the inclusion and exclusion criteria, please refer to the ADNI protocol. In addition, we also collected relevant clinical data for this study, including neuroscale information such as MMSE (Mini-Mental State Examination), CDR (Clinical Dementia Rating), and ADAS (Alzheimer's Disease Assessment Scale), as well as clinical information such as age, gender, education level, and APOE4.

### Data preprocessing and feature extraction

In this study, we used the Statistical Parametric Mapping (SPM12 Software—Statistical Parametric Mapping) version V2.5.5 and the Computational Anatomy Toolbox (CAT12) version r1109 as data postprocessing analysis tools based on the MATLAB platform. The specific steps followed the SPM12 user manual written by Ashburner et al. [11] and the CAT12 user manual written by Gaser et al. [12]. After topology correction, spherical expansion, and spherical registration, the structural MRI data obtained the central cortex map. Based on the graph, multiple cortical indicators are extracted. In VBM, the volume morphological features of different brain regions, such as cortical volume, are extracted. In SBM, thickness morphological features of different brain regions, such as cortical thickness (CT), sulcus depth (SD), gyrification index (GI), and fractal dimension (FD), are extracted. Finally, we computed a total of 778 features, including 170 VBM features and 608 SBM features. Details of the relevant indicators and corresponding brain areas can be found in the auxiliary materials.

Fig. 1 Study flowchart



### Feature reduction and radiomics signature construction

To exclude unreproducible, redundant, and irrelevant features from the extracted VBM and SBM feature sets in the training set, we used variance, minimum redundancy maximum relevance (mRMR), least absolute shrinkage and selection operator (LASSO), and gradient boosting decision tree (GBDT) ensemble reduction methods for feature reduction. Then the SVM algorithm was used to construct a morphological biomarker based on the remaining features from the two feature sets. In this study, we named it the radiomics signature (RS). In addition, the SVM algorithm based on the training queue uses a cross-validation procedure, including an external loop with repeated random splitting of the training queue into training subgroups and test subgroups. A total of 50 random splits are used to evaluate the classification performance. The other is the inner loop of fivefold cross-validation used to optimize the hyperparameters of the algorithm. We selected the model with the highest accuracy to build PS, and the score value calculated based on RS for each case reflects the probability of MCI progressing to AD. These score values are named rad-scores. The accuracy of RS was evaluated in the training and test sets using the area under the receiver operating characteristic (ROC) curve, and calibration curves were used to evaluate whether the imaging biomarkers were overfitted. The detailed steps of feature reduction and machine learning are described in the supplementary material.

### Construction and validation of the combinatorial model

We used the reverse stepwise selection method based on the Akaike information criterion (AIC) stopping rule to select independent predictive factors from the clinical features and RS in the training set and constructed a combinatorial model based on this foundation by multiple factor logistic regression. To verify the improvement in model performance after including RS, we evaluated the performance of different independent predictive factors using the area under the ROC curve. In addition, we used the DeLong test to determine the differences between the combinatorial model and other independent predictive factors. Finally, we calculated the risk values for each patient progressing to AD based on the model and then divided the training, test, and entire cohorts into low- and high-risk groups based on the cutoff value of the training set ROC curve. The number of patients who actually progressed from MCI to AD was compared between the low- and high-risk groups. We used the Hosmer–Lemeshow test to analyze the goodness of fit of the combinatorial model and used calibration curves to intuitively evaluate the consistency between the predicted pMCI probability and the actual pMCI probability.

### Statistical analysis

All statistical analyses were performed using MedCalc software (V.11.2; 2011 MedCalc Software bvba, Mariakerke,

Belgium), SPSS software 17.0 (IBM, Armonk, NY), Graph-Pad (San Diego, CA), and R software (version 3.4.1; <http://www.rproject.org>). The Kolmogorov–Smirnov test was used to evaluate the normality of variable distributions. The continuous variables were compared by performing a two-sample *t* test or Mann–Whitney *U* test, and the categorical variables were compared by a Chi-square test. All statistics were two way, and the statistical significance was set at  $P < 0.05$ .

## Result

### Comparison of clinical factors

All clinical data between the training set and test set were not statistically significant ( $P > 0.05$ ). There were statistically significant differences ( $P < 0.05$ ) in CDR and ADAS scores between the stable and progressive MCI groups in the training set and test set. Additionally, there was a statistically significant difference ( $P < 0.05$ ) in MMSE scores between the stable and test groups in the training set, while the other clinical data had no statistically significant differences ( $P > 0.05$ ), as shown in Table 1.

### Construction and validation of the radiomics signature

After feature dimensionality reduction, three features were retained, including one voxel morphological feature and two surface morphological features: hippocampal volume, island-short-circuit index of the insula, and folding of the

superior parietal gyrus. The RS constructed based on these three features showed good predictive performance in both the training and testing sets. The AUC values were 0.865 and 0.826, and the specificity values were 0.903 and 0.747, respectively. The sensitivity values were 0.773 and 0.900, and the calibration curve showed that the RS did not exhibit overfitting. In addition, there was a significant difference in rad-score between the training and testing sets, as shown in Fig. 2.

### Construction and validation of the combinatorial model

Based on stepwise logistic regression analysis, APOE4, ADAS scores, and RS were identified as independent predictors of pMCI, and a combinatorial model was constructed, as shown in Table 2. The Hosmer–Lemeshow test showed that the combinatorial model did not overfit ( $P > 0.05$ ), and the calibration curve demonstrated that the predictive performance of the combinatorial model was consistent with the actual pMCI status. The ROC curve showed that the AUC of the combinatorial model was 0.945 and 0.867 in the training and testing groups, respectively, with a sensitivity of 0.909 and 0.900 and a specificity of 0.823 and 0.747. The probability of progression to AD for each patient based on the combinatorial model showed significant differences in both the training and testing groups ( $P < 0.05$ ) (Fig. 3). The DeLong test showed that the diagnostic performance of the combined model was significantly different from that of the independent predictor APOE4 ( $P < 0.05$ ) and the independent predictor ADAS in the testing set ( $P < 0.05$ ), but there was

**Table 1** Comparison and analysis of clinical data between the training and test sets

Characteristics	All cohort ( <i>n</i> = 121)	Training cohort ( <i>n</i> = 84)			Test cohort ( <i>n</i> = 37)			Training cohort vs. Test cohort <i>P</i> value
		MCI stable ( <i>n</i> = 62)	MCI progress ( <i>n</i> = 22)	<i>P</i> value	MCI stable ( <i>n</i> = 27)	MCI progress ( <i>n</i> = 10)	<i>P</i> value	
Gender ( <i>n</i> , %)								
Male	73 (60.33)	40(64.51)	10 (45.45)	0.096	15 (55.55)	8 (80.00)	0.197	0.785
Female	48 (39.67)	22(35.49)	12 (54.55)		12 (44.45)	2 (20.00)		
APOE4 ( <i>n</i> , %)								
Negative	56 (46.28)	35(56.45)	5 (22.72)	0.127	13 (48.15)	3 (30.00)	0.175	0.656
Positive	65 (53.72)	27(43.55)	17 (77.28)		14 (51.85)	7 (70.00)		
Age (year)	72.74 ± 7.3	72.04 ± 7.32	75.23 ± 5.72	0.068	71.78 ± 7.72	74.15 ± 8.65	0.428	0.133
MMSE (score)	27.88 ± 1.65	28.03 ± 1.62	26.86 ± 1.58	0.004*	28.48 ± 1.52	27.50 ± 1.43	0.087	0.994
CDRS (score)	1.37 ± 0.78	1.23 ± 0.78	1.80 ± 0.75	0.004*	1.16 ± 0.60	1.80 ± 0.78	0.013*	0.780
ADAS (score)	9.65 ± 4.61	8.43 ± 3.72	13.30 ± 5.27	<0.001*	8.33 ± 3.18	12.70 ± 6.07	0.007*	0.833
PTEDUCAT (year)	15.88 ± 2.68	15.79 ± 2.85	16.18 ± 2.70	0.576	15.89 ± 2.19	15.70 ± 3.09	0.836	0.918

ADAS Alzheimer's Disease Assessment Scale, APOE4 apolipoprotein E 4, CDR Clinical Dementia Rating Scale, MMSE Mini-Mental State Examination

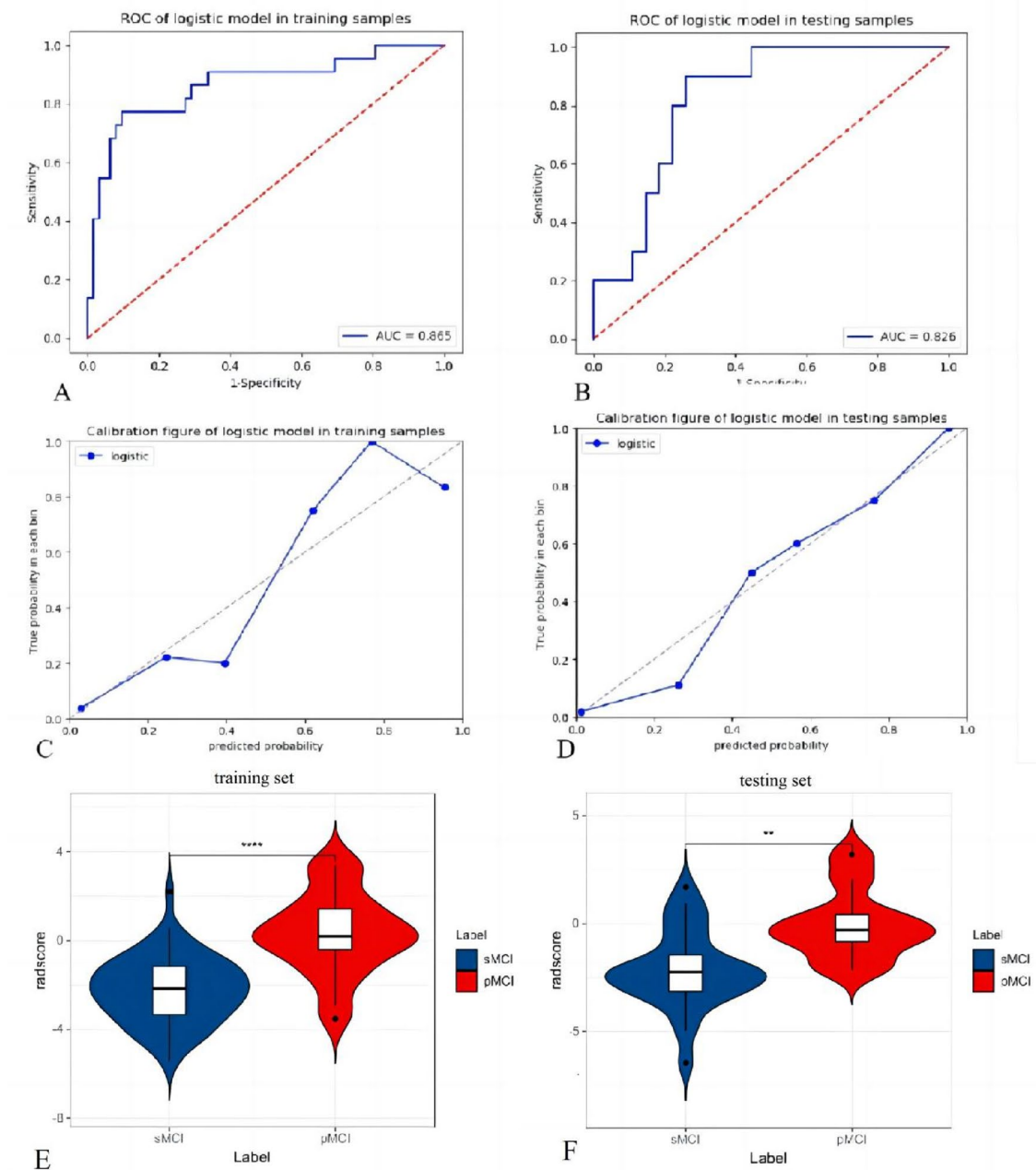


**Fig. 2** Panels **A** and **B** show the diagnostic performance of RS in the training set (left) and testing set (right), respectively. Panels **C** and **D** show the calibration curves of RS in the training set (left) and testing set (right), respectively. Panels **E** and **F** show statistically significant differences in model scores between pMCI and sMCI observed in the training set (left) and testing set (right) for the imaging biomarker.

Red represents sMCI, and blue represents pMCI. Asterisks (\*) indicate a significance level of  $p < 0.001$ , the black horizontal line represents the median, and the upper and lower boundaries of the white box represent the upper and lower quartiles of the dataset (color figure online)

no significant difference for other independent predictors (Table 3 and Fig. 4). Using the optimal cutoff value of 0.46329, patients were divided into low-risk and high-risk groups, and there was a significant difference in the number of MCI progressors between the low- and high-risk

groups in the training set, testing set, and entire cohort ( $P < 0.05$ ) (Fig. 5).

**Table 2** Selection of independent predictors

Variable	Univariate logistic regression		Multivariate logistic regression	
	OR (95% CI)	<i>P</i> value	OR (95% CI)	<i>P</i> value
Gender	1.258 (0.555, 2854)	0.583	NA	NA
APOE4	3.512 (1.425, 8.658)	0.006	4.421 (1.240, 15.765)	0.022*
Age (year)	1.060 (0.999, 1.125)	0.054	NA	NA
MMSE	0.666 (0.516, 0.859)	0.002	0.708 (0.493, 1.017)	0.062
CDRS	2.619 (1.513, 4.532)	0.001	NA	NA
ADAS	1.276 (1.142, 1.426)	0.000	1.157 (1.017, 1.317)	0.026*
PTEDUCAT	1.030 (0.885, 1.199)	0.701	NA	NA
RS	2.443 (1.715, 3.480)	0.000	303.471 (28.942, 3182.065)	<0.001*

ADAS Alzheimer's Disease Assessment Scale, APOE4 apolipoprotein E4, CDR Clinical Dementia Rating Scale, RS radiomics signature, CI confidence interval, MMSE Mini-Mental State Examination, OR odds ratio

\* indicates  $P < 0.05$

## Discussion

In this study, we established a RS using a combination of VBM and SBM models. We found significant differences in imaging biomarker scores between patients with sMCI and pMCI, indicating that a combination of voxel-based and surface-based morphometric biomarkers of the entire brain cortex could potentially serve as an imaging feature to identify patients progressing from pMCI to AD. Furthermore, the use of machine learning methods to combine imaging biomarkers, APOE4, and ADAS scores further improved predictive performance, potentially providing a useful tool for clinically identifying individuals at high risk for AD.

Several studies have already demonstrated that measurements of cortical morphology can serve as markers for MCI severity or progression. The combination of VBM and SBM for measuring the volume and thickness of the entire brain cortex in structural MRI reflects progression in pMCI. Wu [13] and Long [14] separately investigated the progression mechanism of pMCI using whole-brain cortical VBM and SBM, respectively, and found that the areas with reduced volume were located in the hippocampus, adjacent to the hippocampus, amygdala, cingulate gyrus, angular gyrus, and frontal lobe, while the areas with decreased cortical thickness were located in the frontal, temporal, parietal lobes, and cingulate gyrus. Their studies also found hippocampal volume, the island short gyrus cortical folding index in the insula, and the cortical folding index in the posterior cingulate gyrus. Therefore, our study provides new insights into the morphological evaluation of the cortex.

According to our research results, RS extracted using morphological measurement techniques has good diagnostic efficiency in discriminating between pMCI and sMCI, which may reflect the main pathological changes in the brain cortex associated with pMCI progression. This may be related to radiological features such as hippocampal

volume, island short gyrus folding index, and superior parietal gyrus folding index, which are associated with the conversion from pMCI to AD. Studies have shown that the reduction of hippocampal volume is one of the biomarkers of early Alzheimer's disease (AD), which may involve many biological processes, such as cell death, inflammatory response, and neurotransmitter imbalance. The measurement of hippocampal volume can assist in the early diagnosis of AD, monitoring the progress of disease and evaluating the therapeutic effect [15]. Therefore, the results of this study suggest that the protection of hippocampal formation may help to delay the development of AD. In addition, the insular short gyrus is a region of the cerebral cortex, which is involved in the functions of language, attention, memory, and cognitive control. The fold index of the insular short gyrus cortex reflects the complexity and folding degree of the cerebral cortex, which may be related to the connection density of neurons and information processing. Measuring the fold index of the short insular gyrus can help early diagnose and predict whether mild cognitive impairment (MCI) will progress to AD [16]. In addition, the fold index of the short insular gyrus may be related to different types of cognitive impairment, which is of great significance for understanding the damage pattern and predicting the potential of cognitive function recovery. Parieto occipital gyrus is a part of cerebral cortex, which is involved in attention, working memory, and spatial cognition. The fold index of parieto-occipital cortex reflects the folding degree of cerebral cortex, which may be related to the connection of neurons, information transmission, and the progress of AD [17]. These studies also further confirm the results of this study. The results of Dang [18] and Garg [19] confirmed gray matter changes and hippocampal degeneration in the early detection of MCI and Alzheimer's disease. Cho [20] found that the excessive accumulation of tau

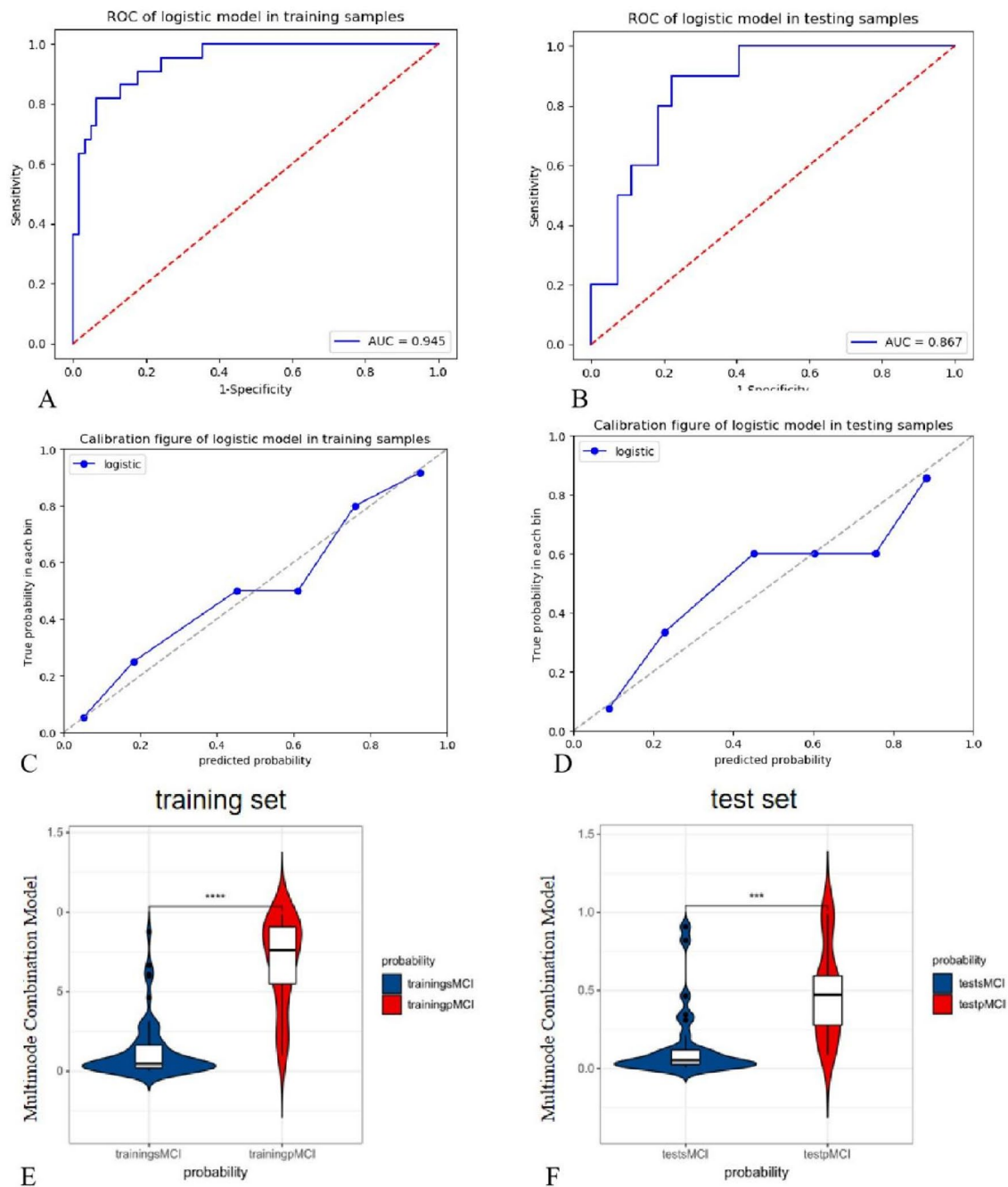


**Fig. 3** Panels **A** and **B** show the diagnostic performance of the multimodal combination model in the training set (left) and testing set (right), respectively. Panels **C** and **D** display the calibration curves of the multimodal combination model in the training set (left) and testing set (right), respectively. Panels **E** and **F** show the statistically sig-

nificant differences in model scores between pMCI and sMCI in the training set (left) and testing set (right), respectively. Red represents pMCI, and blue represents sMCI. \*\* indicates  $P < 0.001$ , the red line represents the median, and the white box represents the interquartile range of the dataset (color figure online)

protein in the superior parietal cortex is a characteristic of early-onset Alzheimer's disease, which also supports our research conclusion. In addition, radiological features (island short gyral folding index, superior parietal gyrus folding index) are also involved in the development mechanisms of other diseases. For example, the incidence of

right middle gyrus lesions in deficit schizophrenia [21] is significantly higher than in non-deficit schizophrenia, and changes in the morphology of the superior parietal cortex [22] are also observed in vascular dementia.

To improve the classification and predictive ability of RS in disease, we incorporated clinical information in this

**Table 3** Diagnostic performance comparison of the multimodal combination model, imaging biomarkers, ADAS, and APOE4 in the training and testing sets

Characteristics	Training cohort				Test cohort			
	AUC	Sensitivity	Specificity	<i>P</i> value	AUC	Sensitivity	Specificity	<i>P</i> value
Multimodal combinatorial model	0.945	0.935	0.823	NA	0.867	0.900	0.778	NA
Radiomics signature	0.866	0.773	0.903	0.054 <sup>a</sup>	0.828	0.900	0.747	0.437 <sup>a</sup>
ADAS	0.778	0.773	0.565	0.001 <sup>b*</sup>	0.720	0.500	0.889	0.063 <sup>b*</sup>
APOE4	0.669	0.682	0.774	<i>P</i> < 0.001 <sup>c*</sup>	0.591	0.700	0.481	0.011 <sup>c*</sup>

a, b, and c indicate the comparison of diagnostic performance between the multimodal combination model and RS, ADAS, and APOE4, respectively

\* indicates *P* < 0.05

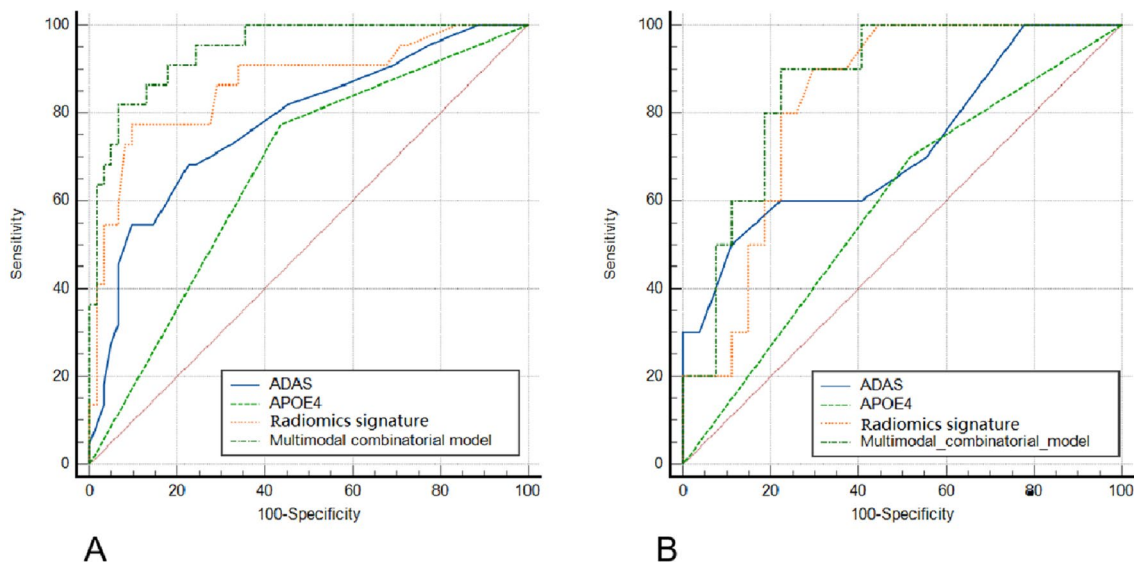


**Fig. 4** Panels **A** and **B** show the ROC curves for the multimodal combination model, RS, APOE4, and ADAS in predicting the progression from pMCI to AD in the training set and testing set, respectively. *AD*

Alzheimer's disease, *ADAS*, Alzheimer's Disease Assessment Scale, *APOE4* apolipoprotein E4

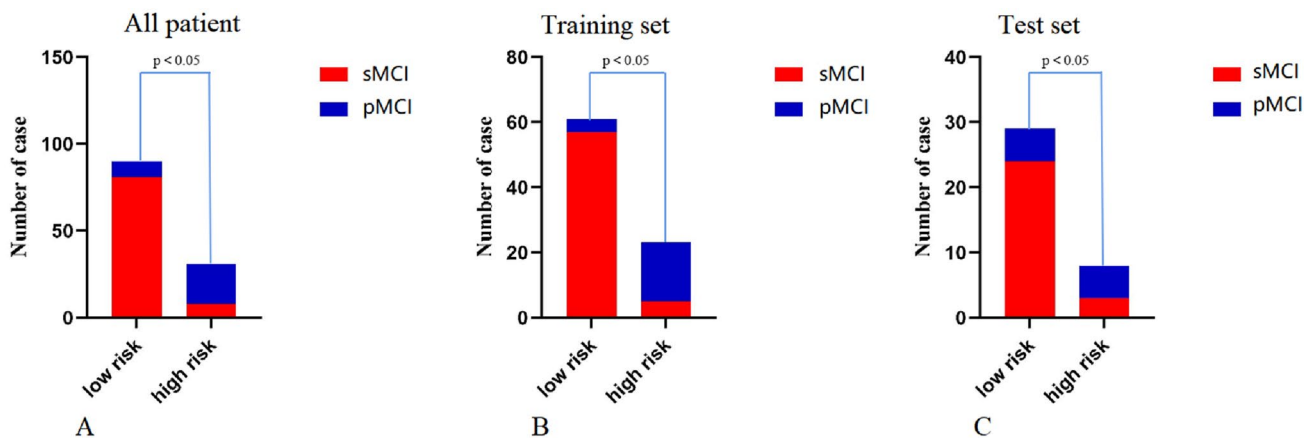


**Fig. 5** Panels **A**, **B**, and **C** show the performance of the multimodal combination model in different risk classifications in the entire cohort, training, and testing sets, respectively. Red represents sMCI, and blue represents pMCI (color figure online)

study. While cerebrospinal fluid  $\beta$  and tau-amyloid proteins (AUC = 0.927) have significant advantages in AD detection, they are invasive and cannot be widely applied in clinical practice. The features used in our study are all noninvasive. Currently, the most commonly used tool both domestically and internationally is the MMSE. Our study also showed that the MMSE is an independent predictor of MCI disease progression, but it was not included in the model construction, which may further indicate that the MMSE is not sensitive for identifying mild cognitive impairment (MCI) [23]. In addition, we found that the ADAS score was included as an independent predictor in the model, which also demonstrated that the ADAS score is more comprehensive and specific in evaluating MCI patients. Moreover, in the study by Ben Jemaa S et al. on AD [24, 25], they compared the ADAS-Cog, MMSE, and Clinical Dementia Rating Scale (CDR) and found that the ADAS-Cog (AUC = 0.92) exhibited the best detection ability, which is consistent with our study results. Furthermore, the APOE4 gene [26] may be a potential target for gene therapy in AD patients, and the above conclusion is further confirmed by APOE4 as a feature of the model in this study.

The research findings of Shu [27] demonstrated that when combined with clinical factors, the AUC value for predicting MCI progression based on radiological features increased from 0.714 to 0.824. Our study also supports this conclusion, as the diagnostic efficiency of our prediction model increased from 0.82 to 0.93 after incorporating ADAS and APOE4, which may have been due in part to the use of machine learning modeling. Previous studies have shown that Hu et al. [28] achieved an AUC of 0.815 and sensitivity of 0.8 for classifying sMCI and pMCI using a deep learning model. Our model achieved an AUC of 0.841 and sensitivity of 0.90, which is significantly higher than Hu's results, indicating that even multimodal combination models are more effective than single modality models.

However, there are limitations to our study. First, it is a single-center study, and the influence of data from different sources or collection domains may affect the MRI data, which often suffer from domain shift problems. Second, this is a retrospective study without further longitudinal prospective research. Finally, future model construction that includes more dimensions of features will be necessary to predict the mechanism of pMCI using comprehensive models that only include a few main clinical features. We hope that more data and longitudinal studies in the future can verify the results of this study.

In summary, the current research supports our hypothesis that radiological features based on cortical measurements of the entire brain can distinguish between pMCI and sMCI. The application of a comprehensive model that combines radiological features with clinical information and machine learning will be an important method for managing

progressive MCI patients and may help provide personalized treatment strategies in clinical practice.

**Supplementary Information** The online version contains supplementary material available at <https://doi.org/10.1007/s40520-023-02456-1>.

**Funding** This work was funded by National Natural Science Foundation of China, 82101983, Yuan Shao.

## Declarations

**Conflict of interest** All authors disclosed no relevant relationships.

**Ethical approval** All procedures performed in studies involving human participants were in accordance with the ethical standards of the institutional and/or national research committee and with the 1964 Helsinki declaration and its later amendments or comparable ethical standards.

**Informed consent** For this type of study formal consent is not required.

## References

- Kang L, Jiang J, Huang J et al (2020) Identifying early mild cognitive impairment by multi-modality MRI-based deep learning. *Front Aging Neurosci* 12:206
- Tang L, Wu X, Liu H et al (2021) Individualized prediction of early Alzheimer's disease based on magnetic resonance imaging radiomics, clinical, and laboratory examinations: a 60-month follow-up study. *J Magn Reson Imaging* 54:1647–1657
- Gomersall T, Smith SK, Blewett C et al (2017) It's definitely not Alzheimer's: perceived benefits and drawbacks of a mild cognitive impairment diagnosis. *Br J Health Psychol* 22:786–804
- Gao Y, Wee CY, Kim M et al (2015) MCI identification by joint learning on multiple MRI data. *Med Image Comput Comput Assist Interv* 9350:78–85
- Fjell AM, Walhovd KB (2010) Structural brain changes in aging: courses, causes and cognitive consequences. *Rev Neurosci* 21:187–221
- Schmitter D, Roche A, Maréchal B et al (2014) An evaluation of volume-based morphometry for prediction of mild cognitive impairment and Alzheimer's disease. *Neuroimage Clin* 7:7–17
- Mechelli A, Crinion JT, Noppeney U et al (2004) Neurolinguistics: structural plasticity in the bilingual brain. *Nature* 431:757
- Goto M, Abe O, Hagiwara A et al (2022) Advantages of using both voxel- and surface-based morphometry in cortical morphology analysis: a review of various applications. *Magn Reson Med* 21:41–57
- Ma Z, Jing B, Li Y et al (2020) Identifying mild cognitive impairment with random forest by integrating multiple MRI morphological metrics. *J Alzheimers Dis* 73:991–1002
- Lee G, Nho K, Kang B et al (2021) Predicting Alzheimer's disease progression using multi-modal deep learning approach. *Sci Rep* 2019:9
- Ashburner J, Friston KJ (2000) Voxel-based morphometry—the methods. *Neuroimage* 11:805–821
- Dahnke R, Yotter RA, Gaser C (2013) Cortical thickness and central surface estimation. *Neuroimage* 15:336–348
- Wu Z, Peng Y, Hong M et al (2021) Gray matter deterioration pattern during Alzheimer's disease progression: a regions-of-interest based surface morphometry study. *Front Aging Neurosci* 13:593898

14. Long Z, Huang J, Li B et al (2018) A comparative atlas-based recognition of mild cognitive impairment with voxel-based morphometry. *Front Neurosci* 12:916
15. Den Heijer T, van der Lijn F, Koudstaal PJ et al (2010) A 10-year follow-up of hippocampal volume on magnetic resonance imaging in early dementia and cognitive decline. *Brain* 133:1163–1172
16. Núñez C, Callén A, Lombardini F et al (2020) Alzheimer's disease neuroimaging initiative. Different cortical gyrification patterns in Alzheimer's disease and impact on memory performance. *Ann Neurol* 88:67–80
17. Ten Kate M, Dicks E, Visser PJ et al (2018) Alzheimer's Disease Neuroimaging Initiative. Atrophy subtypes in prodromal Alzheimer's disease are associated with cognitive decline. *Brain* 141:3443–3456
18. Dang M, Yang C, Chen K et al (2023) Beijing aging brain rejuvenation initiative, for the Alzheimer's disease neuroimaging initiative. Hippocampus-centred grey matter covariance networks predict the development and reversion of mild cognitive impairment. *Alzheimers Res Ther* 15:27
19. Garg N, Choudhry MS, Bodade RM (2023) A review on Alzheimer's disease classification from normal controls and mild cognitive impairment using structural MR images. *J Neurosci Methods* 384:109745
20. Cho H, Choi JY, Lee SH et al (2017) Excessive tau accumulation in the parieto-occipital cortex characterizes early-onset Alzheimer's disease. *Neurobiol Aging* 53:103–111
21. Takahashi T, Sasabayashi D, Takayanagi Y et al (2022) Gross anatomical features of the insular cortex in schizophrenia and schizotypal personality disorder: potential relationships with vulnerability, illness stages, and clinical subtypes. *Front Psychiatry* 13:1050712
22. Jones RS, Waldman AD (2004) 1H-MRS evaluation of metabolism in Alzheimer's disease and vascular dementia. *Neurol Res* 26:488–495
23. Manero RM, Casals-Coll M, Sánchez-Benavides G et al (2014) Diagnostic validity of the Alzheimer's disease functional assessment and change scale in mild cognitive impairment and mild to moderate Alzheimer's disease. *Dement Geriatr Cogn Disord* 37:366–375
24. Wessels AM, Dowsett SA, Sims JR (2018) Detecting treatment group differences in Alzheimer's disease clinical trials: a comparison of Alzheimer's disease assessment scale—cognitive subscale (ADAS-Cog) and the clinical dementia rating—sum of boxes (CDR-SB). *J Prev Alzheimers Dis* 5:15–20
25. Ben Jemaa S, Attia Romdhane N, Bahri-Mrabet A et al (2017) An Arabic version of the cognitive subscale of the Alzheimer's disease assessment scale (ADAS-Cog): reliability, validity, and normative data. *J Alzheimers Dis* 60:11–21
26. Blanchard JW, Akay LA, Davila-Velderrain J et al (2022) APOE4 impairs myelination via cholesterol dysregulation in oligodendrocytes. *Nature* 611:769–779
27. Shu Z, Xu Y, Shao Y et al (2020) Radiomics from magnetic resonance imaging may be used to predict the progression of white matter hyperintensities and identify associated risk factors. *Eur Radiol* 30:3046–3058
28. Hu Z, Wang Z, Jin Y et al (2023) VGG-TSwinformer: transformer-based deep learning model for early Alzheimer's disease prediction. *Comput Methods Programs Biomed* 229:107291

**Publisher's Note** Springer Nature remains neutral with regard to jurisdictional claims in published maps and institutional affiliations.